ISSN: 2152-1972

The IRM
Quarterly
Summer 2013, Vol. 23 No.2

Inside...

Some Like it Hot! A new high temperature MFM comes online at the IRM

Dario Bilardello and Mike Jackson
IRM

Applications of different magnetic imaging techniques are becoming increasingly popular in the study of rock magnetism. “Seeing magnetism” undoubtedly provides better understanding of known phenomena and discovery of important new ones. To this extent, a variety of techniques involving different underlying principles exist, allowing observations at room, low and high temperatures:

Magnetic force microscopy (MFM) allows imaging micromagnetic features that are 10’s of nanometers in scale, using thin-sections or polished surfaces of natural samples. The origins of magnetic remanence can thus be investigated at the nanoscale, within single grains.

Optical techniques such as Bitter, magneto-optical Kerr effect (MOKE) and TEM-based techniques (electron holography, Lorentz microscopy) have also been used to image magnetic structures in natural materials and synthetic analogues. While each of these imaging techniques has advantages and disadvantages related to resolution, ease of use and flexibility, almost all of them are confined to room T observations due to various technical limitations of the existing systems.

Exceptions to this have been attempts to image low-T micromagnetic structures in the monoclinic phase of magnetite (T<122 K) using prototype instruments (e.g., LT MFM Moloni et al, 1996) or transmission electron microscopes equipped with cooling stages (e.g., Kasama et al. 2012). Magnetic imaging above room-T has been confined to low-resolution optical techniques either using the Bitter technique to investigate MD particles (10-50 µm) of magnetite and titanomagnetite up to T~600 K, or with MOKE to study mm-sized single crystals of magnetite up to the Curie temperature ~850 K (e.g., Muxworthy and Williams 2006).

Here at the IRM we have had a room-temperature MFM since 1992. Its primary uses have been to investigate the internal structures of domain walls and domains, the relationship between mineral microstructures and magnetic domain configurations in natural and synthetic (titano)magnetites in varying remanent states, magnetization structures in silicate-hosted inclusions and oxidized titanomagnetites, and the effects of shock remagnetization

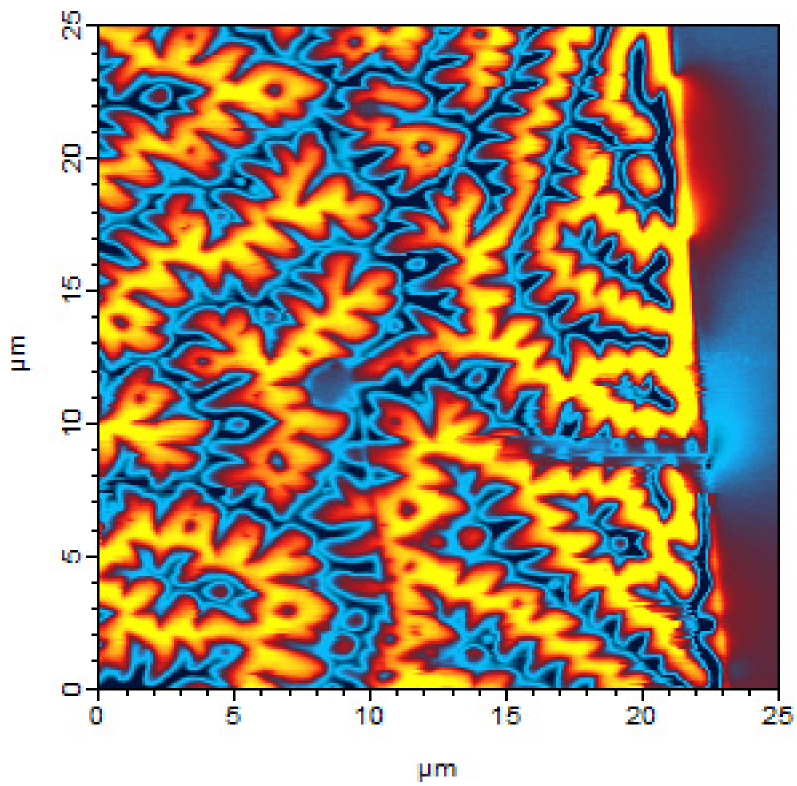

Fig 1. A magnetic image of a Mount St. Helens Ti-magnetite acquired on the new MFM

on domain states in iron sulfides.

However, many advances have been made in MFM instrumentation over the past 20 years, including the possibility of making observations over a range of controlled temperatures: the latest generation MFMs are outfitted with environmental stages for precise heating and cooling in controlled atmospheres up to T= 650-700 K (377-427° C) which allow a variety of important rock-magnetic processes to be studied directly in single grains. Furthermore, MFM samples are usually in a form suitable for reflected light, EM and microprobe analyses, allowing complementary chemical, compositional, and structural characterizations on the same grains imaged magnetically.

We are very proud to introduce one such new generation MFM, an Asylum Research MFP-3D MFM, to our quiver of magnetic imaging instrumentation. Together with our old MFM, and the Bitter and MOKE capabilities, the new MFM will improve our (and our guests’) ability

cont’d. on pg. 10...

Visiting Fellows' Reports

Gegham Style: Applying Obsidian Magnetic Studies in Central Armenia

Ellery Frahm
Department of Archaeology, University of Sheffield
e.frahm@sheffield.ac.uk

The Gegham highlands in central Armenia encompass more than a hundred Quaternary volcanoes, including a series of archaeologically significant obsidian sources. In particular, the extensive Gutansar complex was the volcanic origin of most obsidian artifacts discovered at two sites recently excavated by the Hrazdan Gorge Palaeolithic Project, a collaboration including the University of Connecticut's Palaeolithic Studies Lab and Armenia's Institute of Archaeology and Ethnography. Using portable X-ray fluorescence, I analyzed 1700 obsidian artifacts from Lower Palaeolithic Nor Geghi-1 and Middle Palaeolithic Lusakert-1. Based on the artifacts' elemental "fingerprints," 93% were matched to the Gutansar volcanic complex.

For hundreds of millennia, early humans used obsidian available from flows, domes, and intrusions scattered across more than 80 km2 around Gutansar. However, any patterns that could reveal how past peoples used the different obsidian outcrops are currently invisible. Obsidian is chemically homogeneous throughout this complex. Thus, traditional chemical sourcing methods cannot discern obsidian from different areas of the Gutansar complex.

My research at the IRM uses the magnetic properties of Gutansar obsidian as a means to identify patterns in stone tools crucial to reconstruct settlement, subsistence, and other behaviors during the Palaeolithic.

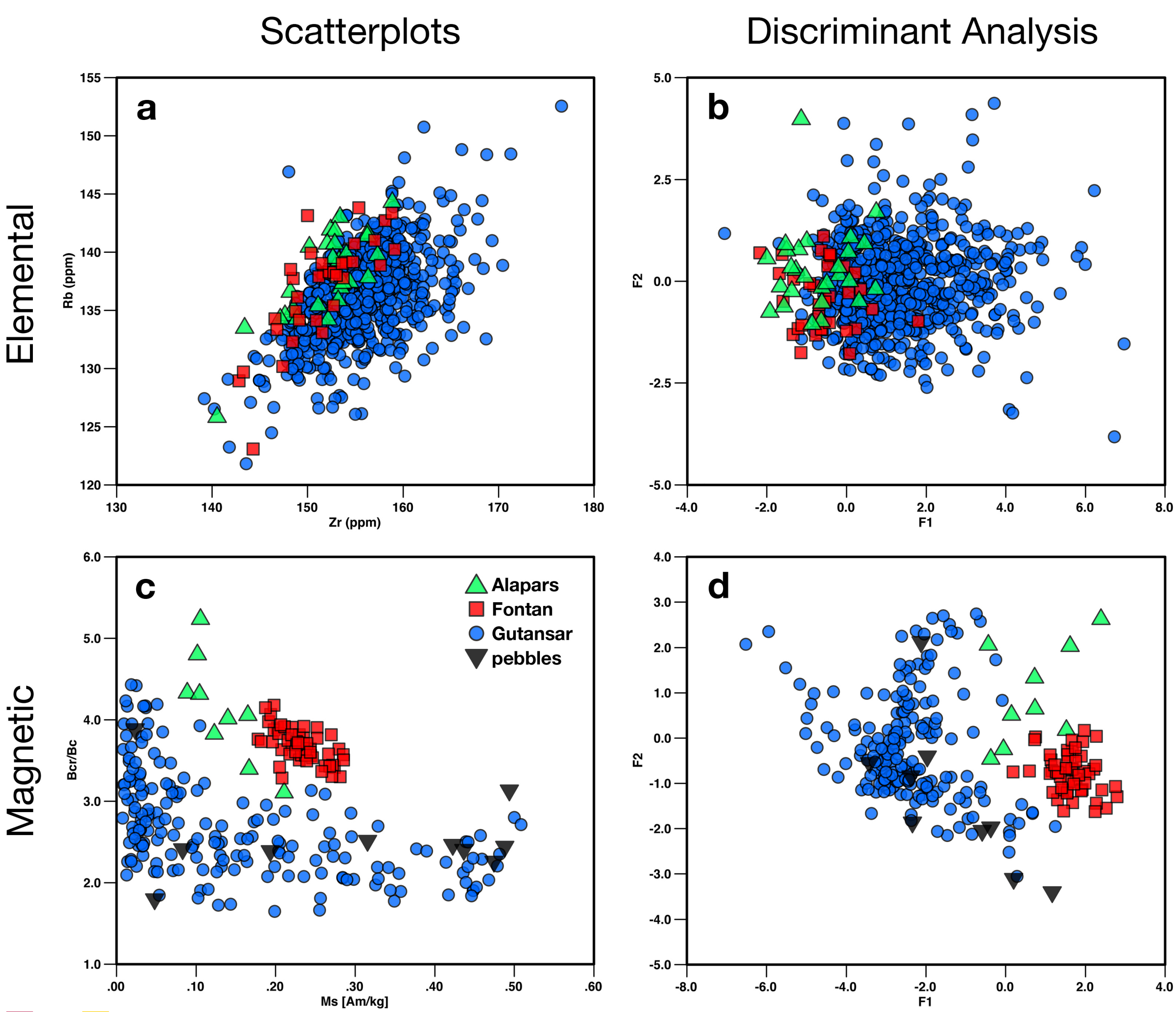

Without distinguishing obsidian tools from varied parts of this complex, we are left with a largely incomplete picture of early human activities due to missing information about resource acquisition in the Gegham highlands. My work seeks to remedy the gap by using magnetic properties to recognize different quarrying sites. Pilot studies in Turkey and California have established the validity of this approach (Frahm and Feinberg 2013).

The pioneering work of McDougall et al. (1983) used NRM, Mr, and χ to match obsidian artifacts to their origins, albeit with mixed success. My preliminary work showed that hysteresis parameters (Bc, Bcr, Mr, Ms) can discern not only obsidian flows that are geochemically identical but also different quarries within a flow. The parameters reflect differences in compositions, sizes and shapes of magnetic grains in obsidian. At the IRM in July, I acquired hysteresis loops and backfield curves for 250 specimens from 25 Gutansar sampling locations.

The plots here show some of my initial results. Plots A and B demonstrate that obsidian from three volcanic centers at this complex -- Fontan, Alapars, and Gutansar proper -- cannot be discerned by elemental composition. Magnetic hysteresis parameters, however, can differentiate them. Plots C and D show that hysteresis parameters largely separate the three volcanic centers, and they reveal that obsidian pebbles found at Nor Geghi-1 match the Gutansar flow rather than the Fontan and Alapars domes. Other data show that different portions of the Fontan dome have obsidian with distinct magnetic properties, enabling quarry identification.

Because magnetic properties of obsidian vary on scales different from geochemistry, their measurement may reveal previously unnoticed patterns in lithic assemblages. The ultimate goal uncovering new insights about human behavior in the Gegham highlands.

References

Frahm, E., and J.M. Feinberg. 2013. From Flow to Quarry: Magnetic Properties of Obsidian and Changing the Scales of Archaeological Sourcing. Journal of Archaeological Science 40(10):3706-3721. http://dx.doi.org/10.1016/j.jas.2013.04.029

McDougall, J.M., D.H. Tarling, and S.E. Warren. 1983. The Magnetic Sourcing of Obsidian Samples from Mediterranean and Near Eastern Sources. Journal of Archaeological Science 10(5):441-452. http://dx.doi.org/10.1016/0305-4403(83)90059-6

The next Visiting Fellowship application deadline is October 30, 2013.

Current Articles

A list of current research articles dealing with various topics in the physics and chemistry of magnetism is a regular feature of the IRM Quarterly. Articles published in familiar geology and geophysics journals are included; special emphasis is given to current articles from physics, chemistry, and materials-science journals. Most are taken from ISI Web of Knowledge, after which they are subjected to Procrustean culling for this newsletter. An extensive reference list of articles (primarily about rock magnetism, the physics and chemistry of magnetism, and some paleomagnetism) is continually updated at the IRM. This list, with more than 10,000 references, is available free of charge. Your contributions both to the list and to the Current Articles section of the IRM Quarterly are always welcome.

Anisotropy and Magnetic Fabrics

Garcia-Lasanta, C., B. Oliva-Urcia, T. Roman-Berdiel, A. M. Casas, and F. Perez-Lorente (2013), Development of magnetic fabric in sedimentary rocks: insights from early compactional structures, Geophysical Journal International, 194(1), 182-199.

Inoue, J., H. Itoh, M. A. Tanaka, K. Mibu, T. Niizeki, H. Yanagihara, and E. Kita (2013), Study of Perpendicular Magnetic Anisotropy and Magneto-Elastic Coupling in the First Principles and Phenomenology, Ieee Transactions on Magnetics, 49(7), 3269-3272.

Lamali, A., N. Merabet, B. Henry, S. Maouche, K. Graine-Tazerout, A. Mekkaoui, and M. Ayache (2013), Polyphased geodynamical evolution of the Ougarta (Algeria) magmatic complexes evidenced by paleomagnetic and AMS studies, Tectonophysics, 588, 82-99.

Lenhardt, N., H. Bohnel, M. Hinderer, and J. Hornung (2013), Paleocurrent direction measurements in a volcanic setting by means of anisotropy of magnetic susceptibility: A case study from the Lower Miocene Tepoztlan Formation (Transmexican Volcanic Belt, Central Mexico), Sedimentary Geology, 290, 1-14.

Lesic, V., E. Marton, V. Cvetkov, and D. Tomic (2013), Magnetic anisotropy of Cenozoic igneous rocks from the Vardar zone (Kopaonik area, Serbia), Geophysical Journal International, 193(3), 1182-1197.

Archeomagnetism

Ao, H., M. J. Dekkers, Q. Wei, X. K. Qiang, and G. Q. Xiao (2013), New evidence for early presence of hominids in North China, Scientific Reports, 3.

Koleini, F., L. C. Prinsloo, M. H. A. Schoeman, I. Pikirayi, and S. Chirikure (2013), Characterization of the corrosion layer on iron archaeological artefacts from K2 (825-1220 AD), an archaeological site in South Africa, Studies in Conservation, 58(3), 274-282.

Vaughn, K. J., H. Van Gijseghem, M. L. Grados, and J. W. Eerkens (2013), hematite mining on the south coast of Peru: archaeological investigations at Mina Primavera, Chungara-Revista De Antropologia Chilena, 45(1), 131-142.

Bio(geo)magnetism

Bazylinski, D. A., et al. (2013), Magnetovibrio blakemorei gen. nov., sp nov., a magnetotactic bacterium (Alphaproteobacteria: Rhodospirillaceae) isolated from a salt marsh, International Journal of Systematic and Evolutionary Microbiology, 63,

1824-1833.
Chao, Y., P. P. Karmali, R. Mukthavaram, S. Kesari, V. L. Kouznetsova, I. F. Tsigelny, and D. Simberg (2013), Direct Recognition of Superparamagnetic Nanocrystals by Macrophage Scavenger Receptor SR-AI, Acs Nano, 7(5), 4289-4298.
Dziuba, M. V., T. V. Kolganova, V. M. Gorlenko, and B. B. Kuznetsov (2013), Species diversity of magnetotactic bacteria from the Ol'khovka River, Russia, Microbiology, 82(3), 335-340.
Perez-Gonzalez, T., C. Valverde-Tercedor, A. Yebra-Rodriguez, T. Prozorov, M. T. Gonzalez-Munoz, J. M. Arias-Penalver, and C. Jimenez-Lopez (2013), Chemical Purity of Shewanella oneidensis-Induced Magnetites, Geomicrobiology Journal, 30(8), 731-748.
Prodan, A. M., S. L. Iconaru, C. M. Chifiriuc, C. Bleotu, C. S. Ciobanu, M. Motelica-Heino, S. Sizaret, and D. Predoi (2013), Magnetic Properties and Biological Activity Evaluation of Iron Oxide Nanoparticles, Journal of Nanomaterials.

Books

Frankel, H. R. (2012), The Continental Drift Controversy: Paleomagnetism and Confirmation of Drift, Cambridge, Cambridge University Press, Vols I-IV.
Hinze, W. J., R. R. B. von Frese, and A. H. Saad (2013) Gravity and Magnetic Exploration: Principles, Practices, and Application. Cambridge, Cambridge University Press, 525 pp.

Chronostratigraphy/Magnetostratigraphy

Al-Ramadan, K., and E. El-Khoriby (2013), Integrated diagenesis and sequence stratigraphic study of tidal sandstones: the Adedia Formation (Cambro-Ordovician), Sinai, Egypt, Arabian Journal of Geosciences, 6(6), 2009-2020.
Costa, E., M. Garces, M. Lopez-Blanco, J. Serra-Kiel, G. Bernaola, L. Cabrera, and E. Beamud (2013), The Bartonian-Priabonian marine record of the eastern South Pyrenean foreland basin (NE Spain): a new calibration of the larger foraminifers and calcareous nannofossil biozonation, Geologica Acta, 11(2), 177-+.
Cuenca-Bescos, G., J. Rofes, J. M. Lopez-Garcia, H. A. Blain, R. Rabal-Garces, V. Sauque, J. L. Arsuaga, J. M. B. de Castro, and E. Carbonell (2013), The small mammals of Sima del Elefante (Atapuerca, Spain) and the first entrance of Homo in Western Europe, Quaternary International, 295, 28-35.
Deng, C. L., H. Y. He, Y. X. Pan, and R. X. Zhu (2013), Chronology of the terrestrial Upper Cretaceous in the Songliao Basin, northeast Asia, Palaeogeography Palaeoclimatology Palaeoecology, 385, 44-54.
Dzyuba, O. S., O. P. Izokh, and B. N. Shurygin (2013), Carbon isotope excursions in Boreal Jurassic-Cretaceous boundary sections and their correlation potential, Palaeogeography Palaeoclimatology Palaeoecology, 381, 33-46.
Geist, E. L., J. D. Chaytor, T. Parsons, and U. ten Brink (2013), Estimation of submarine mass failure probability from a sequence of deposits with age dates, Geosphere, 9(2), 287-298.
Gibert, L., G. R. Scott, P. Montoya, F. J. Ruiz-Sanchez, J. Morales, L. Luque, J. Abella, and M. Leria (2013), Evidence for an African-Iberian mammal dispersal during the pre-evaporitic Messinian, Geology, 41(6), 691-694.
Goguitchaichvili, A., M. T. Ramirez-Herrera, M. Calvo-Rathert, B. A. Reyes, A. Carrancho, C. Caballero, F. Bautista, and J. M. Contreras (2013), Magnetic fingerprint of tsunami-induced deposits in the Ixtapa-Zihuatanejo Area, Western Mexico, International Geology Review, 55(12), 1462-1470.
Guo, Y. Q., C. C. Huang, J. L. Pang, X. C. Zha, Y. L. Zhou, Y. Z. Zhang, and L. Zhou (2013), Sedimentological study of the stratigraphrat the site of Homo erectus yunxianensis in the upper Hanjiang River valley, China, Quaternary International, 300, 75-82.
Ivanov, A. V., H. Y. He, L. K. Yan, V. V. Ryabov, A. Y. Shevko, S. V. Palesskii, and I. V. Nikolaeva (2013), Siberian Traps large igneous province: Evidence for two flood basalt pulses around the Permo-Triassic boundary and in the Middle Triassic, and contemporaneous granitic magmatism, Earth-Science Reviews, 122, 58-76.
Lallier, F., C. Antoine, J. Charreau, G. Caumon, and J. Ruiu (2013), Management of ambiguities in magnetostratigraphic correlation, Earth and Planetary Science Letters, 371, 26-36.
Manzi, V., R. Gennari, F. Hilgen, W. Krijgsman, S. Lugli, M. Roveri, and F. J. Sierro (2013), Age refinement of the Messinian salinity crisis onset in the Mediterranean, Terra Nova, 25(4), 315-322.
Nilsson, A., Y. S. Lee, I. Snowball, and M. Hill (2013), Magnetostratigraphic importance of secondary chemical remanent magnetizations carried by greigite (Fe3S4) in Miocene sediments, New Jersey shelf (IODP Expedition 313), Geosphere, 9(3), 510-520.
Srivastava, S. K., and D. R. Braman (2013), The palynostratigraphy of the Edmonton Group (Upper Cretaceous) of Alberta, Canada, Palynology, 37(1), 1-27.
Tori, F., and S. Monechi (2013), Lutetian calcareous nannofossil events in the Agost section (Spain): implications toward a revision of the Middle Eocene biomagnetostratigraphy, Lethaia, 46(3), 293-307.
Toro-Moyano, I., et al. (2013), The oldest human fossil in Europe, from Orce (Spain), Journal of Human Evolution, 65(1), 1-9.
Wan, X. Q., J. Zhao, R. W. Scott, P. J. Wang, Z. H. Feng, Q. H. Huang, and D. P. Xi (2013), Late Cretaceous stratigraphy, Songliao Basin, NE China: SK1 cores, Palaeogeography Palaeoclimatology Palaeoecology, 385, 31-43.
Wu, H. C., S. H. Zhang, G. Q. Jiang, T. S. Yang, J. H. Guo, and H. Y. Li (2013), Astrochronology for the Early Cretaceous Jehol Biota in northeastern China, Palaeogeography Palaeoclimatology Palaeoecology, 385, 221-228.
Zhang, W. L., X. M. Fang, C. H. Song, E. Appel, M. D. Yan, and Y. D. Wang (2013), Late Neogene magnetostratigraphy in the western Qaidam Basin (NE Tibetan Plateau) and its constraints on active tectonic uplift and progressive evolution of growth strata, Tectonophysics, 599, 107-116.

Computation and Development

Ionita, V., L. Petrescu, A. Bordianu, and O. Tabara (2013), Efficient Use of Preisach Hysteresis Model in Computer Aided Design, Advances in Electrical and Computer Engineering, 13(2), 121-126.
Sagnotti, L. (2013), Demagnetization Analysis in Excel (DAIE). An open source workbook in Excel for viewing and analyzing demagnetization data from paleomagnetic discrete samples and u-channels, Annals of Geophysics, 56(1).
Voigt, J., S. Knappe-Gruneberg, A. Schnabel, R. Korber, and M. Burghoff (2013), Measures to reduce the residual field and field gradient inside a magnetically shielded room by a factor of more than 10, Metrology and Measurement Systems, 20(2), 239-248.
Vrijsen, N. H., J. W. Jansen, J. C. Compter, and E. A. Lomonova (2013), Measurement method for determining the magnetic hysteresis effects of reluctance actuators by evaluation of the force and flux variation, Review of Scientific Instruments, 84(7).
Wang, B. Y., and S. L. Qu (2013), Discrete dipole approximation simulations of absorption spectra and local electric field

distributions of superparamagnetic magnetite nanoparticles, Laser Physics, 23(4).

Environmental Magnetism and Climate

Baumgart, P., U. Hambach, S. Meszner, and D. Faust (2013), An environmental magnetic fingerprint of periglacial loess: Records of Late Pleistocene loess-palaeosol sequences from Eastern Germany, Quaternary International, 296, 82-93.

Chakarova, K., V. Rusanov, and A. X. Trautwein (2013), Study of deep sea Fe-Mn sediments and the possibility to use these formations as paleoclimatic indicator, Journal of Atmospheric and Solar-Terrestrial Physics, 99, 143-149.

Dewangan, P., N. Basavaiah, F. K. Badesab, A. Usapkar, A. Mazumdar, R. Joshi, and T. Ramprasad (2013), Diagenesis of magnetic minerals in a gas hydrate/cold seep environment off the Krishna-Godavari basin, Bay of Bengal, Marine Geology, 340, 57-70.

El-Hasan, T., and M. Lataifeh (2013), Field and dual magnetic susceptibility proxies for heavy metal pollution assessment in the urban soil of Al-Karak City, South Jordan, Environmental Earth Sciences, 69(7), 2299-2310.

Geirsdottir, A., G. H. Miller, D. J. Larsen, and S. Olafsdottir (2013), Abrupt Holocene climate transitions in the northern North Atlantic region recorded by synchronized lacustrine records in Iceland, Quaternary Science Reviews, 70, 48-62.

Gu, Y. S., X. Y. Huang, W. G. Zhang, H. L. Hong, and Y. T. Li (2013), Red Palaeosols Development in Response to the Enhanced East Asia Summer Monsoon since the Mid-Pleistocene in South China: Evidence Derived from Magnetic Properties and Molecular Fossil Records, Journal of Earth Science, 24(3), 382-396.

Han, G. Z., and G. L. Zhang (2013), Changes in magnetic properties and their pedogenetic implications for paddy soil chronosequences from different parent materials in southChina, European Journal of Soil Science, 64(4), 435-444.

Hatfield, R. G., J. S. Stoner, A. E. Carlson, A. V. Reyes, and B. A. Housen (2013), Source as a controlling factor on the quality and interpretation of sediment magnetic records from the northern North Atlantic, Earth and Planetary Science Letters, 368, 69-77.

Hong, H. L., C. W. Wang, K. F. Zeng, Y. S. Gu, Y. B. Wu, K. Yin, and Z. H. Li (2013), Geochemical constraints on provenance of the mid-Pleistocene red earth sediments in subtropical China, Sedimentary Geology, 290, 97-108.

Howard, J. L., B. R. Dubay, and W. L. Daniels (2013), Artifact weathering, anthropogenic microparticles and lead contamination in urban soils at former demolition sites, Detroit, Michigan, Environmental Pollution, 179, 1-12.

Hu, P. X., Q. S. Liu, J. Torrent, V. Barron, and C. S. Jin (2013), Characterizing and quantifying iron oxides in Chinese loess/paleosols: Implications for pedogenesis, Earth and Planetary Science Letters, 369, 271-283.

Jia, J., D. S. Xia, B. Wang, S. Zhao, G. H. Li, and H. T. Wei (2013), The investigation of magnetic susceptibility variation mechanism of Tien Mountains modern loess: Pedogenic or wind intensity model?, Quaternary International, 296, 141-148.

Jordanova, D., N. Jordanova, and U. Werban (2013), Environmental significance of magnetic properties of Gley soils near Rosslau (Germany), Environmental Earth Sciences, 69(5), 1719-1732.

Ketrot, D., A. Suddhiprakarn, I. Kheoruenromne, and B. Singh (2013), Interactive effects of iron oxides and organic matter on charge properties of red soils in Thailand, Soil Research, 51(3), 222-231.

Kim, W., S. J. Doh, Y. Yu, and Y. I. Lee (2013), Magnetic evaluation of sediment provenance in the northern East China Sea using fuzzy c-means cluster analysis, Marine Geology, 337, 9-19.

Li, H. Y., S. H. Zhang, H. C. Wu, K. L. Zhao, T. S. Yang, and L. Zhao (2013), Rock magnetic records of the Qingshankou Formation of SK-1 south borehole in Songliao Basin, Northeast China, and their paleoclimate implications, Palaeogeography Palaeoclimatology Palaeoecology, 385, 71-82.

Liu, W. M., and L. Y. Zhang (2013), Chemical magnetization in Chinese loess, Physics of the Earth and Planetary Interiors, 218, 14-18.

Liu, Y., Z. F. He, and Z. H. Wang (2013), Magnetic properties of Holocene core ZK9 in the subaqueous Yangtze delta and their mechanisms and implications, Frontiers of Earth Science, 7(3), 331-340.

Ma, M. M., X. M. Liu, P. P. Hesse, B. Lu, X. L. Guo, and J. S. Chen (2013), Magnetic properties of loess deposits in Australia and their environmental significance, Quaternary International, 296, 198-205.

Nie, J. S., Y. G. Song, J. W. King, R. Zhang, and X. M. Fang (2013), Six million years of magnetic grain-size records reveal that temperature and precipitation were decoupled on the Chinese Loess Plateau during similar to 4.5-2.6 Ma, Quaternary Research, 79(3), 465-470.

Nozawa, T., and M. Fukugita (2013), properties of dust grains probed with extinction curves, astrophysical Journal, 770(1).

Ortega, B., Schaaf, P., Murray, A., Caballero, M., Lozano, S., Ramirez, A. (2013), Eolian deposition cycles since AD 500 in Playa San Bartolo lunette dune, Sonora, Mexico: Paleoclimatic implications, Aeolian Research, 11, 1-13, ISSN 1875-9637, http://dx.doi.org/10.1016/j.aeolia.2013.06.002.

Qiao, Q. Q., B. C. Huang, C. X. Zhang, J. D. A. Piper, Y. P. Pan, and Y. Sun (2013), Assessment of heavy metal contamination of dustfall in northern China from integrated chemical and magnetic investigation, Atmospheric Environment, 74, 182-193.

Qiao, S. Q., X. F. Shi, J. J. Gao, Y. G. Liu, G. Yang, A. M. Zhu, and K. S. Wang (2013), The distribution and variation of elements in sediments off the Huanghe (Yellow) River mouth, Chinese Journal of Oceanology and Limnology, 31(4), 876-885.

Su, Y. L., X. Gao, Q. S. Liu, J. B. Wang, T. Haberzettl, L. P. Zhu, J. H. Li, Z. Q. Duan, and L. D. Tian (2013), Mineral magnetic study of lacustrine sediments from Lake Pumoyum Co, southern Tibet, over the last 19 ka and paleoenvironmental significance, Tectonophysics, 588, 209-221.

Uchoa, S. C. P., H. A. Victor, and F. M. Freire (2013), effect of sulphur rates and incubation time on the dynamics of sulphur forms in soil, Revista Brasileira De Ciencia Do Solo, 37(3), 678-687.

Vodyanitskii, Y. N. (2013), Dissolution of magnetite and redistribution of heavy metals in urban soils (model experiment), Eurasian Soil Science, 46(6), 635-643.

Zhang, J. H., D. S. Xia, Y. Zhang, and Y. H. Liu (2013), Magnetic investigation of peat sediments from the mountain in Arid Regions, Chinese Journal of Geophysics-Chinese Edition, 56(6), 1974-1984.

Extraterrestrial and planetary magnetism

Bezaeva, N. S., D. D. Badyukov, M. A. Nazarov, P. Rochette, and J. Feinberg (2013), Magnetic properties of the Chelyabinsk meteorite: Preliminary results, Geochemistry International, 51(7), 568-574.

Fernandez, A. B., M. E. McHenry, M. Diaz-Michelena, C. Aroca, and M. Maicas (2013), Data Base of Extraterrestrial Magnetic Minerals, Test and Magnetic Simulation, Ieee Transactions on

Magnetics, 49(7), 3533-3536.
Grenfell, J. L., J. W. Stock, and A. B. C. Patzer (2013), CO-oxidation on surface hematite in hot atmospheres of rocky planets, Planetary and Space Science, 84, 14-19.
Lindgren, P., M. R. Lee, M. R. Sofe, and M. E. Zolensky (2013), Clasts in the CM2 carbonaceous chondrite Lonewolf Nunataks 94101: Evidence for aqueous alteration prior to complex mixing, Meteoritics & Planetary Science, 48(6), 1074-1090.
Markley, R. (2013), Missions to Mars: Reimagining the Red Planet in the Age of Spaceflight, 249-272 pp.
Suavet, C., B. P. Weiss, W. S. Cassata, D. L. Shuster, J. Gattacceca, L. Chan, I. Garrick-Bethell, J. W. Head, T. L. Grove, and M. D. Fuller (2013), Persistence and origin of the lunar core dynamo, Proceedings of the National Academy of Sciences of the United States of America, 110(21), 8453-8458.
Weiss, B. P., and L. T. Elkins-Tanton (2013), Differentiated Planetesimals and the Parent Bodies of Chondrites, in Annual Review of Earth and Planetary Sciences, Vol 41, edited by R. Jeanloz, pp. 529-560.

Magnetic Field Records and Paleointensity Methods

Biggin, A. J., S. Badejo, E. Hodgson, A. R. Muxworthy, J. Shaw, and M. J. Dekkers (2013), The effect of cooling rate on the intensity of thermoremanent magnetization (TRM) acquired by assemblages of pseudo-single domain, multidomain and interacting single-domain grains, Geophysical Journal International, 193(3), 1239-1249.
Cawthorn, R. G., and S. J. Webb (2013), Cooling of the Bushveld Complex, South Africa: Implications for paleomagnetic reversals, Geology, 41(6), 687-690.
de Groot, L. V., T. A. T. Mullender, and M. J. Dekkers (2013), An evaluation of the influence of the experimental cooling rate along with other thermomagnetic effects to explain anomalously low palaeointensities obtained for historic lavas of Mt Etna (Italy), Geophysical Journal International, 193(3), 1198-1215.
De Santis, A., E. Qamili, and G. Cianchini (2013), Repeat-station surveys: implications from chaos and ergodicity of the recent geomagnetic field, Annals of Geophysics, 56(1).
Dominici, G., A. Meloni, A. Di Ponzio, and M. Miconi (2012), Italian Magnetic Network and magnetic reference fields at 2010.0, Annals of Geophysics, 55(6), 1121-1135.
Hejda, P., J. Horacek, and T. Bayer (2012), Secular variation on the territory of the Czech Republic and reduction of the magnetic survey to the epoch 2010.5, Annals of Geophysics, 55(6), 1095-1099.
Herve, G., A. Chauvin, and P. Lanos (2013), Geomagnetic field variations in Western Europe from 1500 BC to 200 AD. Part II: New intensity secular variation curve, Physics of the Earth and Planetary Interiors, 218, 51-65.
Herve, G., A. Chauvin, and P. Lanos (2013), Geomagnetic field variations in Western Europe from 1500BC to 200AD. Part I: Directional secular variation curve, Physics of the Earth and Planetary Interiors, 218, 1-13.
Korte, M., and V. Lesur (2012), Repeat station data compared to a global geomagnetic field model, Annals of Geophysics, 55(6), 1101-1111.
Lhuillier, F., G. Hulot, and Y. Gallet (2013), Statistical properties of reversals and chrons in numerical dynamos and implications for the geodynamo, Physics of the Earth and Planetary Interiors, 220, 19-36.
Lise-Pronovost, A., G. St-Onge, C. Gogorza, T. Haberzettl, M. Preda, P. Kliem, P. Francus, B. Zolitschka, and P. S. Team (2013), High-resolution paleomagnetic secular variations and relative paleointensity since the Late Pleistocene in southern South America, Quaternary Science Reviews, 71, 91-108.
Nevalainen, J., I. G. Usoskin, and A. Mishev (2013), Eccentric dipole approximation of the geomagnetic field: Application to cosmic ray computations, Advances in Space Research, 52(1), 22-29.
Scherbakova, V. V., G. V. Zhidkov, A. V. Latyshev, and V. P. Scherbakov (2013), Estimating the variations in paleointensity from the Siberian traps of Maymecha-Kotui and Norilsk regions, Izvestiya-Physics of the Solid Earth, 49(4), 488-504.
Tarduno, J. A., and R. D. Cottrell (2013), Signals from the ancient geodynamo: A paleomagnetic field test on the Jack Hills metaconglomerate, Earth and Planetary Science Letters, 367, 123-132.

Mineral Physics and Chemistry

Howarth, G. H., S. A. Prevec, and M. F. Zhou (2013), Timing of Ti-magnetite crystallisation and silicate disequilibrium in the Panzhihua mafic layered intrusion: Implications for ore-forming processes, Lithos, 170, 73-89.
Ngo, A. T., J. Richardi, and M. P. Pileni (2013), Crack patterns in superlattices made of maghemite nanocrystals, Physical Chemistry Chemical Physics, 15(26), 10666-10672.
Nie, S., E. Starodub, M. Monti, D. A. Siegel, L. Vergara, F. El Gabaly, N. C. Bartelt, J. de la Figuera, and K. F. McCarty (2013), Insight into Magnetite's Redox Catalysis from Observing Surface Morphology during Oxidation, Journal of the American Chemical Society, 135(27), 10091-10098.

Rock and Mineral Magnetism

Akinci, U. (2013), Hysteresis behavior of the anisotropic quantum Heisenberg model, Physics Letters A, 377(28-30), 1672-1676.
Ali-zade, R. A. (2013), Distribution Function of Magnetite Nanoparticles in Size on the Basis of Moments, Ieee Transactions on Magnetics, 49(6), 2893-2898.
Arras, R., B. Warot-Fonrose, and L. Calmels (2013), Electronic structure near cationic defects in magnetite, Journal of Physics-Condensed Matter, 25(25).
Badekar, A. G., S. J. Sangode, S. K. Ghosh, R. P. Tiwari, D. C. Meshram, J. Malsawma, and P. Lalnuntluanga (2013), Petromineralogic and rock magnetic aspects of clastic sedimentation in the Surma basin, Mizoram, Journal of the Geological Society of India, 82(1), 23-37.
Bowles, J. A., M. J. Jackson, T. S. Berquo, P. A. Solheid, and J. S. Gee (2013), Inferred time- and temperature-dependent cation ordering in natural titanomagnetites, Nature Communications, 4.
Burn, D. M., and D. Atkinson (2013), Suppression of Walker breakdown in magnetic domain wall propagation through structural control of spin wave emission, Applied Physics Letters, 102(24).
Burzuri, E., F. Luis, O. Montero, B. Barbara, R. Ballou, and S. Maegawa (2013), Quantum Interference Oscillations of the Superparamagnetic Blocking in an Fe-8 Molecular Nanomagnet, Physical Review Letters, 111(5).
Cava, C. E., L. S. Roman, and C. Persson (2013), Effects of native defects on the structural and magnetic properties of hematite alpha-Fe2O3, Physical Review B, 88(4).
Deng, H. D., and H. Li (2013), Interaction and assembly of non-magnetic spheres and magnetic nanoparticles dispersed in magnetic fluid, Acta Physica Sinica, 62(12).
Dzian, S. A., and B. A. Ivanov (2013), Collective oscillations of the magnetic moments of a chain of spherical magnetic

nanoparticles with uniaxial magnetic anisotropy, Journal of Experimental and Theoretical Physics, 116(6), 975-979.
El Goumi, N., M. Jaffal, C. Rolf, C. Grissemann, F. Melcher, A. Kchikach, M. Hibti, and T. Graupner (2013), Rock magnetic study of basic intrusions and massive sulphides in the Hercynian central Jebilets Massif (Occidental-Meseta), Morocco, Arabian Journal of Geosciences, 6(7), 2581-2597.
Eren, M., and S. Kadir (2013), Colour origin of red sandstone beds within the Hudai Formation (Early Cambrian), Aydincik (Mersin), southern Turkey, Turkish Journal of Earth Sciences, 22(4), 563-573.
Ferguson, R. M., A. P. Khandhar, C. Jonasson, J. Blomgren, C. Johansson, and K. M. Krishnan (2013), Size-Dependent Relaxation Properties of Monodisperse Magnetite Nanoparticles Measured Over Seven Decades of Frequency by AC Susceptometry, Ieee Transactions on Magnetics, 49(7), 3441-3444.
Granata, C., R. Russo, E. Esposito, A. Vettoliere, M. Russo, A. Musinu, D. Peddis, and D. Fiorani (2013), Magnetic properties of iron oxide nanoparticles investigated by nanoSQUIDs, European Physical Journal B, 86(6).
Groschner, C., S. Lan, A. Wise, A. Leary, M. S. Lucas, C. Park, D. E. Laughlin, M. Diaz-Michelena, and M. E. McHenry (2013), The Role of Atmosphere on Phase Transformations and Magnetic Properties of Ulvospinel, Ieee Transactions on Magnetics, 49(7), 4273-4276.
Hari, M., K. Wang, S. J. Bending, E. Arac, D. Atkinson, S. Lepadatu, J. S. Claydon, and C. H. Marrows (2013), Current-driven domain wall motion in artificial magnetic domain structures, Journal of the Korean Physical Society, 62(10), 1534-1538.
Hayward, T. J., and D. A. Allwood (2013), magnetic domain walls traps with potential, Nature Nanotechnology, 8(6), 391-392.
Holzinger, D., N. Zingsem, I. Koch, A. Gaul, M. Fohler, C. Schmidt, and A. Ehresmann (2013), Tailored domain wall charges by individually set in-plane magnetic domains for magnetic field landscape design, Journal of Applied Physics, 114(1).
Honecker, D., and A. Michels (2013), Theory of magnetic small-angle neutron scattering of two-phase ferromagnets, Physical Review B, 87(22).
Hrouda, F., J. Pokorny, J. Jezek, and M. Chadima (2013), Out-of-phase magnetic susceptibility of rocks and soils: a rapid tool for magnetic granulometry, Geophysical Journal International, 194(1), 170-181.
Jeffries, J. R., P. Soderlind, H. Cynn, A. Landa, W. J. Evans, S. T. Weir, Y. K. Vohra, and G. H. Lander (2013), Magnetism and structural distortions in uranium sulfide under pressure, Physical Review B, 87(21).
Kudo, K., and Y. Kawaguchi (2013), Magnetic domain growth in a ferromagnetic Bose-Einstein condensate: Effects of current, Physical Review A, 88(1).
Laha, S. S., R. Regmi, and G. Lawes (2013), Structural origin for low-temperature relaxation features in magnetic nanoparticles, Journal of Physics D-Applied Physics, 46(32).
Liu, X. M., B. Lu, P. Y. Li, F. Russell, X. G. Mao, H. Guo, M. M. Ma, and G. Y. Zhao (2013), Effects of heating environments on thermomagnetic behaviors of synthetic maghemite, Chinese Journal of Geophysics-Chinese Edition, 56(5), 1560-1567.
Martinez-Huerta, J. M., J. D. Medina, L. Piraux, and A. Encinas (2013), Configuration dependent demagnetizing field in assemblies of interacting magnetic particles, Journal of Physics-Condensed Matter, 25(22).
Mlynczak, E., P. Luches, S. Valeri, and J. Korecki (2013), NiO/Fe(001): Magnetic anisotropy, exchange bias, and interface structure, Journal of Applied Physics, 113(23). Morup, S., E. Brok, and C. Frandsen (2013), Spin Structures in Magnetic Nanoparticles, Journal of Nanomaterials. Article ID 720629, 8 pages
Oravova, L., Z. Y. Zhang, N. Church, R. J. Harrison, C. J. Howard, and M. A. Carpenter (2013), Elastic and anelastic relaxations accompanying magnetic ordering and spin-flop transitions in hematite, Fe2O3 (vol 25, 116006, 2013), Journal of Physics-Condensed Matter, 25(25).
Palasyuk, A., E. Blomberg, R. Prozorov, L. Yue, M. J. Kramer, R. W. McCallum, I. E. Anderson, and S. Constantinides (2013), Advances in Characterization of Non-Rare-Earth Permanent Magnets: Exploring Commercial Alnico Grades 5-7 and 9, Jom, 65(7), 862-869.
Pilkington, M., and M. Beiki (2013), Mitigating remanent magnetization effects in magnetic data using the normalized source strength, Geophysics, 78(3), J25-J32.
Raghunathan, A., P. Klimczyk, and Y. Melikhov (2013), Application of Jiles-Atherton Model to Stress Induced Magnetic Two-Phase Hysteresis, Ieee Transactions on Magnetics, 49(7), 3187-3190.
Rapoport, E., and G. S. D. Beach (2013), Transport dynamics of superparamagnetic microbeads trapped by mobile magnetic domain walls, Physical Review B, 87(17).
Rivoirard, S. (2013), High Steady Magnetic Field Processing of Functional Magnetic Materials, Jom, 65(7), 901-909.
Rodionov, A. A., and N. M. Ignatenko (2013), Dependence of spontaneous magnetization and constants of magnetic anisotropy on the size of nanocrystals, Metal Science and Heat Treatment, 55(1-2), 83-86.
Ryu, K. S., L. Thomas, S. H. Yang, and S. Parkin (2013), Chiral spin torque at magnetic domain walls, Nature Nanotechnology, 8(7), 527-533.
Salazar-Camacho, C., M. Villalobos, M. D. Rivas-Sanchez, J. Arenas-Alatorre, J. Alcaraz-Cienfuegos, and M. E. Gutierrez-Ruiz (2013), Characterization and surface reactivity of natural and synthetic magnetites, Chemical Geology, 347, 233-245.
Samofalov, V. N., D. P. Belozorov, and A. G. Ravlik (2013), Strong stray fields in systems of giant magnetic anisotropy magnets, Physics-Uspekhi, 56(3), 269-288.
Senn, M. S., J. P. Wright, and J. P. Attfield (2013), The verwey phase of magnetite - a long-running mystery in magnetism, Journal of the Korean Physical Society, 62(10), 1372-1375.
Skomski, R., P. Kumar, G. C. Hadjipanayis, and D. J. Sellmyer (2013), Finite-Temperature Micromagnetism, Ieee Transactions on Magnetics, 49(7), 3229-3232.
Skomski, R., P. Manchanda, P. Kumar, B. Balamurugan, A. Kashyap, and D. J. Sellmyer (2013), Predicting the Future of Permanent-Magnet Materials, Ieee Transactions on Magnetics, 49(7), 3215-3220.
Skumiel, A., M. Kaczmarek-Klinowska, M. Timko, M. Molcan, and M. Rajnak (2013), Evaluation of Power Heat Losses in Multidomain Iron Particles Under the Influence of AC Magnetic Field in RF Range, International Journal of Thermophysics, 34(4), 655-666.
Song, N. N., et al. (2013), Interspacing dependence of spin-dependent variable range hopping for cold-pressed Fe3O4 nanoparticles, Journal of Applied Physics, 113(18).
Spalek, D. (2013), Two theorems about Lorentz method for asymmetrical anisotropic regions, Bulletin of the Polish Academy of Sciences-Technical Sciences, 61(2), 399-404.
Spurgeon, S. (2013), Electric field utilized to locally pin magnetic domain walls, Mrs Bulletin, 38(8), 598-598.
Venkatachalapathy, R., R. M. Asanulla, C. Manoharan, and T. Radhakrishna (2013), Rock magnetic and geomagnetic field intensity studies on Megalithic archaeological pottery samples from Tamilnadu, India, Quaternary International, 298, 57-67.
Vereda, F., M. D. Morales, B. Rodriguez-Gonzalez, J. de Vicente, and R. Hidalgo-Alvarez (2013), Control of surface morphology and internal structure in magnetite micropar-

ticles: from smooth single crystals to rough polycrystals, Crystengcomm, 15(26), 5236-5244.
Wang, S. Y., S. Lin, and S. G. Lu (2013), Rock magnetism, iron oxide mineralogy and geochemistry of Quaternary red earth in central China and their paleopedogenic implication, Palaeogeography Palaeoclimatology Palaeoecology, 379, 95-103.
Yamamoto, Y., and K. Park (2013), Metastability for the Blume-Capel model with distribution of magnetic anisotropy using different dynamics, Physical Review E, 88(1).
Yoo, S. C., K. W. Moon, and S. B. Choe (2013), Analytic description of domain-wall deformation caused by the Oersted field in current-driven domain-wall motion, Journal of Magnetism and Magnetic Materials, 343, 234-238.

Paleomagnetism and Tectonics

Angiolini, L., G. Crippa, G. Muttoni, and J. Pignatti (2013), Guadalupian (Middle Permian) paleobiogeography of the Neotethys Ocean, Gondwana Research, 24(1), 173-184.
Archibald, D. B., S. M. Barr, J. B. Murphy, C. E. White, T. G. MacHattie, E. A. Escarraga, M. A. Hamilton, and C. R. M. McFarlane (2013), Field relationships, petrology, age, and tectonic setting of the Late Cambrian-Ordovician West Barneys River Plutonic Suite, southern Antigonish Highlands, Nova Scotia, Canada, Canadian Journal of Earth Sciences, 50(7), 727-745.
Bogdanova, S. V., O. B. Gintov, D. M. Kurlovich, N. V. Lubnina, M. K. M. Nilsson, M. I. Orlyuk, I. K. Pashkevich, L. V. Shumlyanskyy, and V. I. Starostenko (2013), Late Palaeoproterozoic mafic dyking in the Ukrainian Shield of Volgo-Sarmatia caused by rotation during the assembly of supercontinent Columbia (Nuna), Lithos, 174, 196-216.
Campos, C., C. Beck, C. Crouzet, F. Demory, A. Van Welden, and K. Eris (2013), Deciphering hemipelagites from homogenites through anisotropy of magnetic susceptibility. Paleoseismic implications (Sea of Marmara and Gulf of Corinth), Sedimentary Geology, 292, 1-14.
Chandler, M. T., P. Wessel, and W. W. Sager (2013), Analysis of Ontong Java Plateau palaeolatitudes: evidence for large-scale rotation since 123 Ma?, Geophysical Journal International, 194(1), 18-29.
Channell, J. E. T., and D. A. Hodell (2013), Magnetic signatures of Heinrich-like detrital layers in the Quaternary of the North Atlantic, Earth and Planetary Science Letters, 369, 260-270.
Cheng, X., et al. (2013), Paleomagnetic data from the Late Carboniferous-Late Permian rocks in eastern Tibet and their implications for tectonic evolution of the northern Qiangtang-Qamdo block, Science China-Earth Sciences, 56(7), 1209-1220.
Cifelli, F., M. Mattei, H. Rashid, and J. Ghalamghash (2013), Right-lateral transpressional tectonics along the boundary between Lut and Tabas blocks (Central Iran), Geophysical Journal International, 193(3), 1153-1165.
Cordani, U. G., M. M. Pimentel, C. E. G. De Araujo, M. A. S. Basei, R. A. Fuck, and V. A. V. Girardi (2013), was there an ediacaran clymene ocean in central south america?, american journal of science, 313(6), 517-539.
Emmerton, S., A. R. Muxworthy, M. A. Sephton, M. Aldana, V. Costanzo-Alvarez, G. Bayona, and W. Williams (2013), Correlating biodegradation to magnetization in oil bearing sedimentary rocks, Geochimica Et Cosmochimica Acta, 112, 146-165.
Gose, W. A., R. E. Hanson, R. E. Harmer, and E. K. Seidel (2013), Reconnaissance paleomagnetic studies of Mesoproterozoic alkaline igneous complexes in the Kaapvaal craton, South Africa, Journal of African Earth Sciences, 85, 22-30.
Gumsley, A. P., M. O. de Kock, H. M. Rajesh, M. W. Knoper, U. Soderlund, and R. E. Ernst (2013), The Hlagothi Complex: The identification of fragments from a Mesoarchaean large igneous province on the Kaapvaal Craton, Lithos, 174, 333-348.
Gungor, T. (2013), Kinematics of the Central Taurides during Neotethys closure and collision, the nappes in the Sultan Mountains, Turkey, International Journal of Earth Sciences, 102(5), 1381-1402.
Klootwijk, C. (2013), Middle-Late Paleozoic Australia-Asia convergence and tectonic extrusion of Australia, Gondwana Research, 24(1), 5-54.
Maffione, M., A. Morris, and M. W. Anderson (2013), Recognizing detachment-mode seafloor spreading in the deep geological past, Scientific Reports, 3.
Olguin-Villa, A. E., J. R. Vidal-Solano, and J. M. Stock (2013), Petrography, geochemistry, petrofabric and paleomagnetism of the Tuff of San Felipe in the Catavina region, Baja California, Mexico, Revista Mexicana De Ciencias Geologicas, 30(2), 282-298.
Perrin, M., L. M. Alva-Valdivia, M. Lopez-Martinez, J. Rosas-Elguera, M. Benammi, J. A. Gonzalez-Rangel, and P. Camps (2013), Palaeomagnetism of the upper volcanic supergroup, southern part of the Sierra Madre Occidental, Mexico, Geophysical Journal International, 193(3), 1250-1264.
Pilipenko, O. V., and V. M. Trubikhin (2013), Paleomagnetic studies of late pleistocene rocks from the Malyi Kut section (Taman Peninsula, Krasnodar krai), Izvestiya-Physics of the Solid Earth, 49(4), 505-516.
Pisarevsky, S. A., D. P. Gladkochub, K. M. Konstantinov, A. M. Mazukabzov, A. M. Stanevich, J. B. Murphy, J. A. Tait, T. V. Donskaya, and I. K. Konstantinov (2013), Paleomagnetism of Cryogenian Kitoi mafic dykes in South Siberia: Implications for Neoproterozoic paleogeography, Precambrian Research, 231, 372-382.
Pisarevsky, S. A., T. K. Biswal, X. C. Wang, B. De Waele, R. Ernst, U. Soderlund, J. A. Tait, K. Ratre, Y. K. Singh, and M. Cleve (2013), Palaeomagnetic, geochronological and geochemical study of Mesoproterozoic Lakhna Dykes in the Bastar Craton, India: Implications for the Mesoproterozoic supercontinent, Lithos, 174, 125-143.
Roca, E., E. Beamud, M. Rubinat, R. Soto, and O. Ferrer (2013), Paleomagnetic and inner diapiric structural constraints on the kinematic evolution of a salt-wall: The Bicorb-Quesa and northern Navarres salt-wall segments case (Prebetic Zone, SE Iberia), Journal of Structural Geology, 52, 80-95.
Sen, K., K. Tripathi, and A. K. Dubey (2013), Is the North Indian continental margin a Palaeo-proterozoic magmatic arc? Insights from magnetomineralogy and geochemistry of the Wangtu Gneissic Complex, Himachal Lesser Himalaya, Current Science, 104(11), 1527-1533.
Shi, W., S. W. Dong, J. H. Li, M. Tian, and G. L. Wu (2013), Formation of the Moping Dome in the Xuefengshan Orocline, Central China and its Tectonic Significance, Acta Geologica Sinica-English Edition, 87(3), 720-729.
Silveira, E. M., U. Soderlund, E. P. Oliveira, R. E. Ernst, and A. B. M. Leal (2013), First precise U-Pb baddeleyite ages of 1500 Ma mafic dykes from the Sao Francisco Craton, Brazil, and tectonic implications, Lithos, 174, 144-156.
Tait, J., G. Straathof, U. Soderlund, R. E. Ernst, R. Key, S. M. Jowitt, K. Lo, M. E. M. Dahmada, and O. N'Diaye (2013), The Ahmeyim Great Dyke of Mauritania: A newly dated Archaean intrusion, Lithos, 174, 323-332.
Teixeira, W., M. S. D'Agrella, M. A. Hamilton, R. E. Ernst, V. A. V. Girardi, M. Mazzucchelli, and J. S. Bettencourt (2013), U-Pb (ID-TIMS) baddeleyite ages and paleomagnetism of 1.79 and 1.59 Ga tholeiitic dyke swarms, and position of the

Rio de la Plata Craton within the Columbia supercontinent, Lithos, 174, 157-174.
Tomezzoli, R. N., A. E. Rapalini, M. G. L. de Luchi, and C. M. Dopico (2013), Further evidence of widespread Permian remagnetization in the North Patagonian massif, Argentina, Gondwana Research, 24(1), 192-202.
Veselovskiy, R. V., A. A. Arzamastsev, L. I. Demina, A. V. Travin, and S. B. Botsyun (2013), Paleomagnetism, geochronology, and magnetic mineralogy of Devonian dikes from the Kola alkaline province (NE Fennoscandian Shield), Izvestiya-Physics of the Solid Earth, 49(4), 526-547.
Zananiri, I., D. Kondopoulou, S. Dimitriadis, and A. Kilias (2013), Insights into the geotectonic evolution of the southern Rhodope as inferred from a combined AMS, microtextural and paleomagnetic study of the Tertiary Symvolon and Vrondou plutons, Tectonophysics, 595, 106-124.
Zhang, S. H., D. A. D. Evans, H. Y. Li, H. C. Wu, G. G. Jiang, J. Dong, Q. L. Zhao, T. D. Raub, and T. S. Yang (2013), Paleomagnetism of the late Cryogenian Nantuo Formation and paleogeographic implications for the South China Block, Journal of Asian Earth Sciences, 72, 164-177.

Prospecting and Surveying

Hayward, N., R. J. Enkin, L. Corriveau, J. F. Montreuil, and J. Kerswill (2013), The application of rapid potential field methods for the targeting of IOCG mineralisation based on physical property data, Great Bear magmatic zone, Canada, Journal of Applied Geophysics, 94, 42-58.
Myer, D., S. Constable, and K. Key (2013), Magnetotelluric evidence for layered mafic intrusions beneath the Voring and Exmouth rifted margins, Physics of the Earth and Planetary Interiors, 220, 1-10.
Pena, J. A., J. I. Manteca, P. Martinez-Pagan, and T. Teixido (2013), Magnetic gradient map of the mine tailings in Portman Bay (Murcia, Spain) and its contribution to the understanding of the bay infilling process, Journal of Applied Geophysics, 95, 115-120.
Quesnel, Y., J. Gattacceca, G. R. Osinski, and P. Rochette (2013), Origin of the central magnetic anomaly at the Haughton impact structure, Canada, Earth and Planetary Science Letters, 367, 116-122.
Ribeiro, V. B., V. H. A. Louro, and M. S. M. Mantovani (2013), 3D Inversion of magnetic data of grouped anomalies - Study applied to Sao Jose intrusions in Mato Grosso, Brazil, Journal of Applied Geophysics, 93, 67-76.

Synthesis

Cai, J. G., S. Y. Chen, J. Hu, Z. Wang, Y. R. Ma, and L. M. Qi (2013), Top-down fabrication of hematite mesocrystals with tunable morphologies, Crystengcomm, 15(32), 6284-6288.
Morel, M., F. Martinez, and E. Mosquera (2013), Synthesis and characterization of magnetite nanoparticles from mineral magnetite, Journal of Magnetism and Magnetic Materials, 343, 76-81.
Ramalakshmi, M., P. Shakkthivel, M. Sundrarajan, and S. M. Chen (2013), Novel method of room temperature ionic liquid assisted Fe3O4 nanocubes and nanoflakes synthesis, Materials Research Bulletin, 48(8), 2758-2765.
Ristic, M., T. Fujii, H. Hashimoto, I. Opacak, and S. Music (2013), A novel route in the synthesis of magnetite nanoparticles, Materials Letters, 100, 93-97.
Shen, K. H., Y. S. Wang, and Y. Li (2013), One-pot Synthesis of Shape-controlled Fe3O4 Nanocrystals with Alkylsulfonylacetic Acid, Chemistry Letters, 42(5), 479-482.
Yu, Y. T., J. H. Peng, B. G. Liu, G. Chen, and C. Srinivasakannan (2013), Investigation on Preparation of Micro-Sized Hematite Powder from Hydrous Ferrous Sulfate Using Microwave and Conventional Heating, High Temperature Materials and Processes, 32(3), 303-308.
Zhang, X., Y. G. Niu, Y. Li, X. M. Hou, Y. B. Wang, R. Bai, and J. P. Zhao (2013), Synthesis, optical and magnetic properties of alpha-Fe2O3 nanoparticles with various shapes, Materials Letters, 99, 111-114.

Spectroscopy and Microscopy

Barrero, C. A., and K. E. Garcia (2013), New direct method for evaluating recoilless f-factors of two iron-sites in Fe-bearing compounds using Mossbauer spectrometry, Journal of Chemical Physics, 139(3).
de la Figuera, J., L. Vergara, A. T. N'Diaye, A. Quesada, and A. K. Schmid (2013), Micromagnetism in (001) magnetite by spin-polarized low-energy electron microscopy, Ultramicroscopy, 130, 77-81.
El-Ghazaly, A., J. M. Mullenix, R. M. White, and S. X. Wang (2013), Kerr-Imaged Edge-Curling Wall Effects of Narrow Magnetic Cores, Ieee Transactions on Magnetics, 49(7), 4017-4020.
Herve, M., S. Tricot, S. Guezo, G. Delhaye, B. Lepine, P. Schieffer, and P. Turban (2013), Quantitative magnetic imaging at the nanometer scale by ballistic electron magnetic microscopy, Journal of Applied Physics, 113(23).
Jiraskova, Y., A. Hendrych, O. Zivotsky, J. Bursik, T. Zak, I. Prochazka, and D. Janickovic (2013), Surface magneto-optical and Mossbauer observations of Fe-Al, Applied Surface Science, 276, 68-75.
Koike, K. (2013), Spin-polarized scanning electron microscopy, Microscopy, 62(1), 177-191.
Li, H. J., D. Wei, and S. N. Piramanayagam (2013), Optimization of perpendicular magnetic anisotropy tips for high resolution magnetic force microscopy by micromagnetic simulations, Applied Physics a-Materials Science & Processing, 112(4), 985-991.
Liu, Z. J., Y. X. Han, L. G. Han, Y. J. Chen, Y. Q. Ma, and L. Fang (2013), Micro-Raman analysis of the pigments on painted pottery figurines from two tombs of the Northern Wei Dynasty in Luoyang, Spectrochimica Acta Part a-Molecular and Biomolecular Spectroscopy, 109, 42-46.
Mahmoud, H. H. M. (2013), Raman Microscopic Analysis of a Multi-Pigmented Surface from the Theban Tomb (TT277), Luxor, Egypt, Acta Physica Polonica A, 123(4), 782-785.
Prieto, A. C., O. Martinez, J. Souto, M. Avella, and A. Guedes (2013), Study of a tabernacle with a remarkable architectural structure: In situ examination using Raman spectroscopy, Journal of Raman Spectroscopy, 44(8), 1156-1162.
Yin, G., Y. F. Lou, F. Zheng, Z. H. Li, D. P. Wu, J. M. Bai, F. L. Wei, and D. Wei (2013), Studies on Domain Structure of FeCoZr Films From MFM Image by Calculating the Surface Stray Field, Ieee Transactions on Magnetics, 49(7), 3553-3556.

MFM 2013 (continued from pg. 1)

to study the fundamental physics of magnetic behavior at elevated temperatures by direct imaging of domain structures in ambient or applied fields.

The MFP-3D is a significant upgrade to our existing room temperature MFM. Unlike our current MFM that can accommodate samples up to 1 cm in diameter, the new unit can scan much larger samples, up to 10 cm in diameter and 2.5 cm in thickness. This larger sample size can easily accommodate a variety of geological samples such as 1" cores and thin section slides without the "downsizing" necessary to fit our older MFM and will allow a greater range of samples to be studied. The MFP-3D can also collect high-pixel-density images (up to 5k x 5k) with high-speed data capture up to 5 MHz, allowing imaging of large structures and small features in the same image, at rates substantially higher than those of the old instrument. In addition to room-temperature imaging, the MFP-3D also allows high-temperature imaging up to 400° C. This is accomplished with a separate high temperature environmental stage (PolyHeater) that sits on the MFP-3D XY scanning stage. Heating and cooling can be done in air or controlled atmospheres (e.g., He, Ar, CO, etc). Sample temperature can be maintained to better than 0.2° C precision with accuracy to 0.5° C and temperature overshoots less than 0.2° C. All control and measurement functions are fully programmable for custom heating-cooling imaging experiments. The heating stage can be used with standard cantilever holders for heating up to 250° C or Asylum Research PEEK™ cantilever holders for T> 250° C. The cantilevers and tips are made from silicon or silicon nitride while the MFM tips are coated with CoCr and all can be heated to much higher temperatures than 400° C and survive. However, sample size is more restricted for HT imaging with a maximum sample diameter of 20 mm and sample thickness of 2 mm but 8 mm diameter is recommended.

The T range of the new MFM reaches the Curie point of important magnetic minerals such as titanomagnetite and pyrrhotite, enabling observation of phenomena related to full thermoremanence (TRM) acquisition. Partial TRMs, involving heating to temperatures less than the Curie point, are of central importance in paleointensity work and in paleomagnetic overprinting, and the new MFM will provide entirely new ways of studying these as well, in minerals like magnetite. Magnetic mineral alteration via oxidation and reduction can also be examined at the nanometer scale using the controlled atmosphere chamber of the new MFM.

Magnetic Force Microscopy

Magnetic force microscopy is one member of a family of imaging modes collectively called scanning probe microscopy, which also includes the scanning tunneling microscope, atomic force microscope and the scanning SQUID microscope.

Unlike the scanning SQUID microscope, which is designed to map magnetic fields from geological thin sections at ~100 μm resolution to study natural remanent magnetization, the MFM is used to map the fine scaled (~50 nm - 100 μm) micromagnetic structures within ferromagnetic particles.

It was developed in 1987 shortly after the invention of the atomic force microscope (AFM), of which it is a special mode of operation, and is a well-developed technique for high resolution imaging with limited sample preparation and without the need for high vacuum conditions. It has been widely used since the early 1990s in the fundamental research of magnetic materials, as well as the development of magnetic recording components. An introduction to MFM operating principles appeared in the IRM Quarterly soon after our first instrument was acquired (IRMQ v2, n4, 1992). Like the AFM, a sharp tip, a few micrometers long and less than 50 nm in diameter, interacts with the specimens surface forces, therefore mapping the surface topography; the MFM tips are coated with magnetic material to enable mapping of the magnetic stray fields above a sample by scanning above the surface. The ferromagnetic tip is mounted on the free end of a flexible cantilever that is 100-200 μm in length. Minute forces on the magnetic tip are detected by changes in the resonant frequency of the cantilever induced by magnetostatic interactions between the ferromagnetic tip and the sample's stray magnetic field at typical tip-sample separations less than 100 nm. As the tip is scanned across the sample, an image of the inhomogeneous stray magnetic fields deriving from such features as domain walls, vortex structures, and surface termination of domains is produced. The MFM does not provide direct information on the near surface distribution of magnetization. Instead, it is a measure of the local stray field components of micromagnetic structures resulting from the distributions of magnetic poles where the magnetization diverges or has a component normal to the surface. In certain respects this is similar to the classical Bitter decoration technique but with spatial resolutions 1000 times better, and with the ability to distinguish polarity.

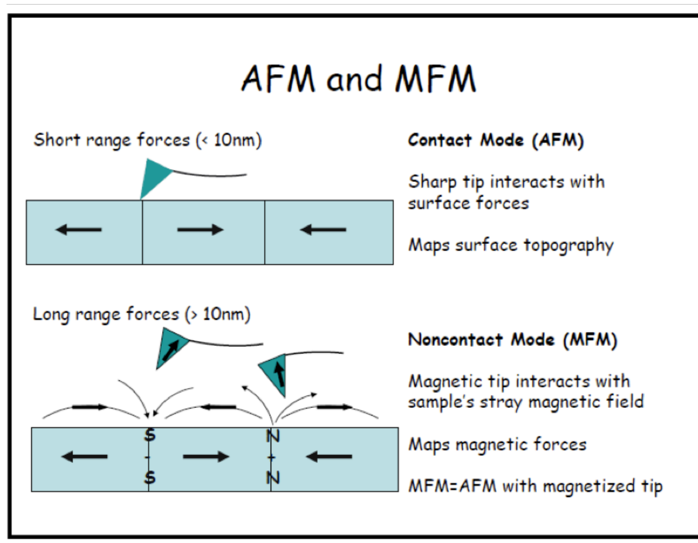

Fig 2. (from Moskowitz, 2008) Vertical gradients of stray field above domain walls exert forces on the tip, attractive or repulsive according to field polarity and tip moment orientation. Vertical force gradients alter the tip oscillation amplitude and phase.

Basics of magnetic contrast information

The following summary is derived largely from the recent review by Ferri et al (2012). The cantilever (incorporating the magnetic tip) is essentially a spring, with a force-displacement constant k=F/z. In the absence of sample-tip interaction forces, the cantilever has a resonant frequency

$$\omega_0 = 2\pi f_0 = \sqrt{\frac{k}{m}}$$

where m is the mass. The cantilever during operation is excited to vibrate close to its resonance frequency, and a laser deflection sensor monitors the tip oscillation amplitude and phase shift with respect to the drive signal.

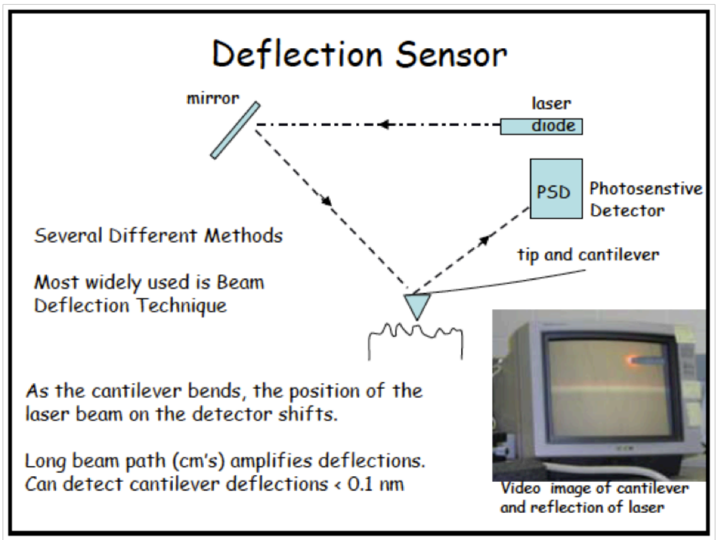

Figure 3. Schematic of an MFM deflection sensor which monitors the tip's oscillation amplitude and phase shift.

When there are probe-sample interaction forces that vary vertically (with vertical derivative dF_i/dz), the effect is equivalent to a change in the cantilever spring constant, $k_{eff} = k - dF_i/dz$. Because the force exerted on a magnetic dipole (like the tip) is proportional to the gradient of the magnetic field, the MFM signal is (to a first approximation) related to the second derivative of the stray field distribution ($dF_i/dz \sim d^2Bz/dz^2$).

An attractive interaction with $dF_i/dz > 0$ will "soften" the cantilever spring, decreasing its resonance frequency:

$$f = f_0 \sqrt{1 - \frac{\partial F_i / \partial z}{k}}$$

Such a shift leads to changes of the oscillation amplitude of the probe and of its phase, which are measurable quantities that can be used to map the lateral variation of dF_i/dz. A common detection method uses the amplitude signal and is referred to as amplitude modulation (AM). The cantilever is driven slightly off resonance (ω_D), where the slope of the amplitude versus frequency curve is high, thus maximizing the signal obtained from a given force derivative (Fig. 4).

The force gradient dF_i/dZ may originate from a range of sources, including long range electrostatic probe-sample interactions (>10 nm, <~100s nm), nanoscale (<10 nm) van der Waals and/or Coulombic Forces, damping, or capillary forces. However, MFM relies on those forces that arise from a long-range (>10 nm) magnetostatic coupling between probe and sample. This coupling is dependent on the internal magnetic structure of the probe, which greatly complicates the mechanism of contrast formation. In general a magnetized body, when brought into the stray field of a sample, will possess magnetic potential energy E:

$$E = -\mu_0 \int \vec{M}_{tip} \cdot \vec{H}_{sample} dV_{tip}$$

where μ_0 is the vacuum permeability. The force acting on a magnetic tip can be calculated by:

$$\vec{F} = -\vec{\nabla} E = \mu_0 \int \vec{\nabla}(\vec{M}_{tip} \cdot \vec{H}_{sample}) dV_{tip}$$

The integration needs to be carried out over the tip volume, or rather its magnetized part.

A limitation of MFM is that the magnetic configuration of the sensing probes is rarely known in detail. It is therefore not possible to model the measured signal from first principles and MFM may generally not be used quantitatively to measure stray fields, let alone magnetization. MFM can, however, be used to compare the experimentally detected stray field variation of a micromagnetic object to that obtained from certain model calculations, or to observe changes that result from applied fields or demagnetization treatments.

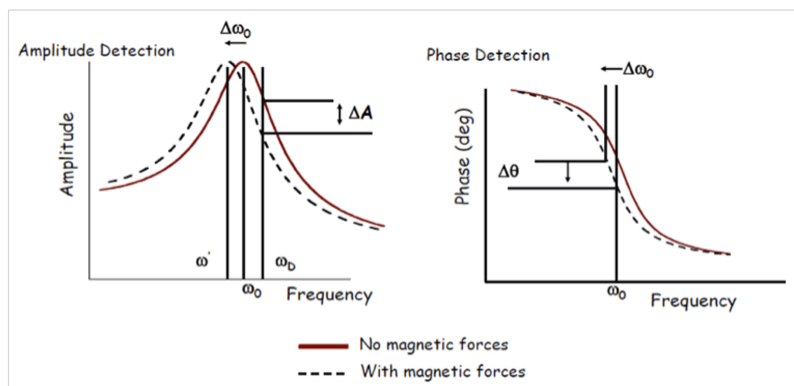

Fig 4. (from Moskowitz, 2008) Changes in the magnetic force on the tip produce changes in resonance frequency, amplitude, and phase of the cantilever oscillations.

Requirements for MFM tips

The cantilever/tip assembly is obviously the critical element of a magnetic force microscope. The tip shape is important due to the long-range nature of magnetic forces. Originally, electrochemically etched wires of cobalt or nickel were used as cantilevers. Thanks to the widespread use of AFM, cantilevers with integrated sharp tips are now fabricated in large numbers out of silicon-based materials. These tips can be coated with a thin layer of magnetic material for the purpose of MFM observations. A lot of effort has been spent on the optimization of magnetic tips in order to obtain quantitative information from MFM data. Coating of conventional tips generates a pattern of magnetic domains, which reduces the effective magnetic moment of the tip. The exact domain structure is unknown and can even change during MFM operation. Nevertheless, some information on the magnetization state of selected probes has been acquired using electron holography.

The spatial resolution in MFM imaging is related to the tip-sample distance, but also to the magnetized part of the tip that is actually exposed to the sample stray field. Thus in order to improve lateral resolution, it is beneficial to restrict the magnetically sensitive region to the smallest possible size. Ideally the effective volume of the probe would consist of a small single-domain ferromagnetic particle located at the probe apex. So-called supertips have been developed based on this idea. However, there is a physical lower limit for the dimensions because an ultra-small particle becomes superparamagnetic, and this limitation becomes more severe for high-temperature operation.

The demand for a strong signal, produced by a small sensitive volume, indicates the need to maximize the magnetic moment in the tip. For this reason a single domain tip will give the best results and is also easier to describe theoretically. Materials with a high saturation magnetization should be used in order to limit the required volume. The well-defined magnetic state of a tip should be stable during scanning and it should interfere as little as possible with the sample's magnetization. A high switching field of the tip can be obtained through the influence of shape anisotropy, which forces the magnetization vector field near the probe apex to align with its axis of symmetry. Ultimately, the smallest detail from which a sufficient signal-to-noise ratio can be gained is determined by the sensitivity of the deflection sensor, as well as the noise characteristics of the cantilever.

Imaging procedure

Different modes of operations of the MFM exist, mainly subdivided under two main categories:
[Constant] Contact mode and Dynamic mode.
In "Contact mode", the probe tip is dragged across the surface of the specimen to 'feel' the topography, this results in high friction and repulsive forces (also the typical AFM mode of operation).
In "Dynamic mode", the probe oscillates flexurally above the surface, "tapping" it as the specimen is scanned. "AC mode", "tapping mode" and "intermittent mode" are trademarked terms for dynamic mode (by Quate/Asylum, Bruker and Topometrics, respectively).
"Dynamic mode" is further subdivided into Attractive mode, where the attractive forces dominate (can be either in contact or non-contact, i.e. the tip oscillates above the specimen either touching/tapping the surface or not) and Repulsive mode, where the repulsive forces dominate (is always in contact).
"Mixed mode" is also a sub-category of "Dynamic mode", which is a switching between "Attractive" and "Repulsive" modes.
Attractive mode broadens the potential well and generates a positive Phase shift, whereas Repulsive mode tightens the potential well and generates a negative Phase shift, therefore generating a sharper image. To get into Repulsive mode it is thus necessary to lower the Phase shift, which is achieved by hitting the surface harder, increasing the free amplitude with respect to the setpoint amplitude. Many other modes of operation also exist, but these are probably the most common.

Quantitative information on the sample stray field can only be derived from MFM images when topographic signal contributions are not included. This is especially important when the tip is brought very close to the sample (in order to improve resolution), since non-magnetic forces become increasingly stronger. The solution to this problem is to keep the topography influence constant by letting the tip follow the surface height profile. This constant distance mode places higher demands on instrument stability, because it is sensitive to drift.

To separate the two signal contributions the tapping-lift method is employed. This involves measuring the topography on a first scan, and the magnetic information during a second scan on the same profile. The difference in height Δh between the two scans, the lift-height, is specified by the user. Topography is measured in dynamic

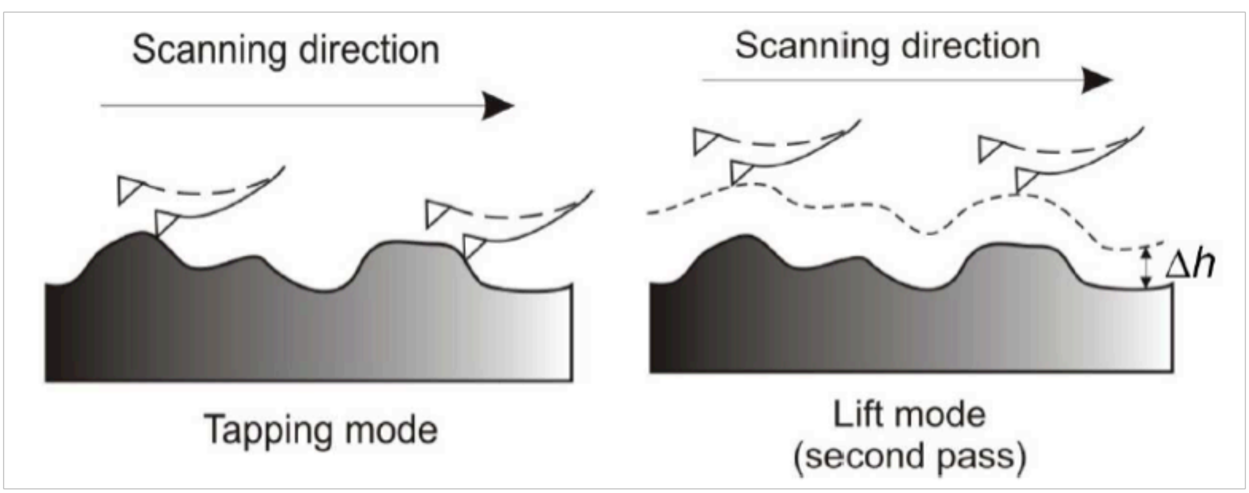

Figure 5: Outline of the lift mode principle. Magnetic information is recorded during the second pass (right panel). The constant height difference between the two scan lines is the lift height Δh.

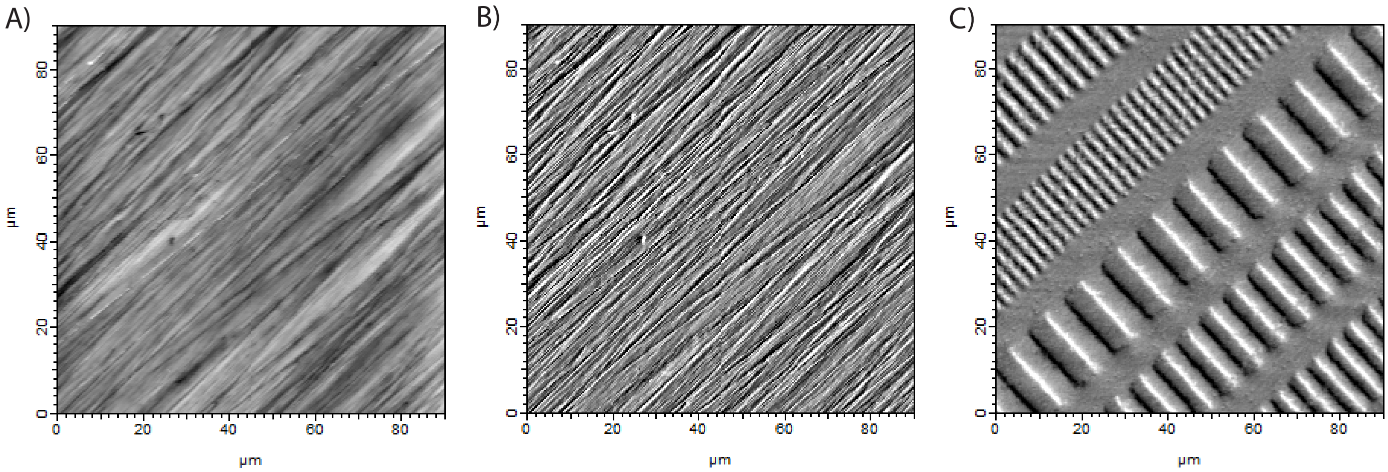

Figure 6: MFM images acquired on a hard drive. A) shows a scan of the topography (tapping mode); in B) another topography image is shown, acquired in tap and lift mode; C) magnetic image with topography subtracted (different sized bits are clearly visible).

amplitude modulation (AM) mode and the data is recorded to one image. This height data is also used to move the tip at a constant local distance above the surface during the second scan, with feedback turned off. Theoretically, topographic contributions are thus eliminated from the second scan image.

Magnetic data can be recorded either as variations in amplitude, frequency or phase of the cantilever oscillation. It is argued that phase detection and frequency modulation give the best results, with higher signal-to-noise ratio.

Examples of new areas of research

The added functionality of the new MFM will greatly improve our abilities in magnetic imaging at room temperatures and will allow us for the first time to systematically study changes in magnetic structures within single and interacting grains at elevated temperatures. This will provide new insights into the acquisition, retention, and alteration of magnetization in nature and will open the way for new and exciting rock magnetic and paleomagnetic discoveries such as the origin and stability of TRM and VRM in MD grains.

Fundamental studies of magnetization at high temperatures (300-800 K) are important, because it is within this temperature range that blocking and acquisition of TRM and VRM occur in nature. Despite many fundamental advances in rock magnetism, the detailed response of micromagnetic structures with respect to time (VRM), temperature (TRM), and chemical change (CRM) and their connections to bulk behavior remain poorly understood for MD materials. For example, major efforts are now underway in retrieving high-resolution, reliable absolute paleointensity data from Precambrian rocks, extraterrestrial materials, and other igneous and archeological materials. It is therefore timely to renew investigations into the temperature and field response of micromagnetic structures most responsible for natural remanent magnetization.

The following is a brief summary of some of the research that can be accomplished with a HT-HFM.

Thermoremanent Magnetization and Paleointensity: The maximum temperatures available so far for MFM imaging (400° C) allow imaging the acquisition of thermoremanent magnetization and the complementary process of thermal demagnetization in many natural samples containing common magnetic minerals such as titanomagnetite, titanohematite, and pyrrhotite. For magnetite-bearing rocks, HT-MFM would still allow to better understand the partial thermal remanent magnetization (pTRM) steps that are used in nearly all Thellier-based paleointensity techniques. One of the major causes of failed paleointensity experiments is associated with samples containing a significant fraction of pseudosingle domain grains that exibit strong pTRM tails during the acquisition of laboratory-induced TRMs. The HT-MFM would allow the study of domain states in such samples, in order to better understand the origin of these pTRM tails.

Thermoremanent Magnetization and Cation Ordering: Very recent work (Bowles et al., 2012) has shown that thermal annealing at relatively low temperatures (350-450° C) can affect the distribution of ferrous and ferric cations in the octahedral and tetrahedral sites of the inverse-spinel structure of intermediate-composition natural titanomagnetites, and thereby cause very significant changes in the Curie temperature without any change in chemical composition or crystallographic structure. Unlike the well-documented similar phenomenon in magnesioferrite (e.g. Harrison and Putnis, 1999a; b), where significant cation reordering occurs only at temperatures hundreds of degrees above the Curie point, these titanomagnetites reorder at temperatures near and even below T_C. This raises very interesting and important questions about how TRM is acquired or demagnetized in a material for which the Curie temperature is not a constant but is itself a function of thermal history.

The ability of the new HT MFM to operate in said temperature range enables to observe the domain configurations associated with different remanent states and different states of cation order, and to gain insight into the micromagnetic processes that operate as the states evolve.

Chemical Remanent Magnetization: CRM is one of the most common forms of remagnetization in nature. Although there have been many experimental studies

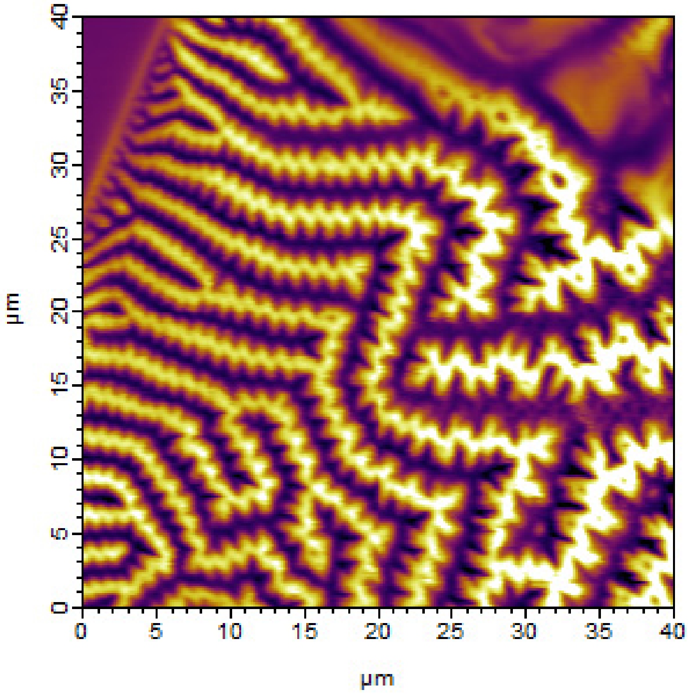

Fig 7. MFM magnetic image of a Mount St. Helens Ti-Magnetite in bright color contrasts.

on CRM in different natural chemical systems, laboratory studies of CRM under controlled conditions are still some of the most challenging experiments in rock magnetism (e.g. Dunlop and Özdemir, 1997). With the exception of the detailed work on hematite-ilmenite intergrowths and lamellar magnetism (McEnroe et al., 2001; Harrison et al., 2002; McEnroe et al., 2008), there has been little work on the direct imaging of micromagnetic structures carrying CRM in other common magnetic minerals (Harrison et al., 2002; Krása et al., 2005) and none at high temperatures where many of these processes occur. It would be possible to use the high-temperature MFM to directly observe the magnetic consequences of incipient oxidation and reduction with controlled time-temperature imaging. These types of experiments will lead to a better understanding of alteration processes that commonly affect rocks in igneous and sedimentary environments as well as during typical laboratory heating protocols for paleointensity measurements.

First Images

Figures 1, 7 and 8 show some of the first results of measurements with the new instrument. All of these are room-T images of homogeneous Al- and Mg- substituted titanomagnetites (~TM30) from Mt. St. Helens (Bowles et al., 2013).

The crystallographic orientations of the imaged particles are unknown, and the high contrast indicates that magnetization is generally oriented at high angles to the surface. Wavy boundaries between the light and dark regions resemble the wall patterns observed in TM60 by Moskwitz et al. (1988).

We are still working on the techniques of high-T specimen preparation and measurement, and "hot" images will be forthcoming!

Acknowledgements

The new MFM was purchased with funding from NSF, grant EAR-1261772

References

Bowles, J. A., M. Jackson, T. S. Berquó, P. A. Sølheid, and J. S. Gee (2012b), Time- and temperature dependent cation ordering in natural titanomagnetites, Nature Communications, 4, 1916 doi:10.1038/ncomms2938.

Dunlop, D. J., and Ö. Özdemir (1997), Rock Magnetism: Fundamentals and Frontiers, 573 pp., Cambridge University Press, Cambridge.

F.A. Ferri, M.A. Pereira-da-Silva and E. Marega Jr. (2012). Magnetic Force Microscopy: Basic Principles and Applications, Atomic Force Microscopy - Imaging, Measuring and Manipulating Surfaces at the Atomic Scale, Dr. Victor Bellitto (Ed.), ISBN: 978-953-51-0414-8, InTech, Available from: http://www.intechopen.com/books/atomic-force-microscopy-imaging-measuring-and-manipulating-surfaces-atthe-atomic-scale/magnetic-force-microscopy-basic-principles-and-applications.

Harrison, R. J., and A. Putnis (1999a), Determination of the mechanism of cation ordering in magnesioferrite (MgFe2O4) from the time- and temperature-dependence of magnetic susceptibility, Phys. Chem. Mineral., 26(4), 322-332, doi: 10.1007/s002690050192.

Harrison, R. J., and A. Putnis (1999b), The magnetic properties and crystal chemistry of oxide spinel solid solutions, Surv. Geophys., 19(6), 461-520, doi: 10.1023/a:1006535023784.

Harrison, R. J., R. E. Dunin-Borkowski, and A. Putnis (2002), Direct imaging of nanoscale magnetic interactions in minerals, Proc. Natl. Acad. Sci. U. S. A., 99(26), 16556-16561.

Kasama, T., R. J. Harrison, N. S. Church, M. Nagao, J. M. Feinberg, and R. E. Dunin-Borkowski (2012), Ferrimagnetic/ferroelastic domain interactions in magnetite below the Verwey transition. Part 1: Electron Holography and Lorentz Microscopy, Phase Transitions: A Multinational Journal, doi: 10.1080/01411594.2012.695373.

Krása, D., V. P. Shcherbakov, T. Kunzmann, and N. Petersen (2005), Self-reversal of remanent magnetization in basalts due to partially oxidized titanomagnetites, Geophys. J. Int., 162(1), 115-136.

McEnroe, S. A., R. J. Harrison, P. Robinson, U. Golla, and M. J. Jercinovic (2001), The effect of finescale microstructures in titanohematite on the acquisition and stability of natural remanent magnetization in granulite facies metamorphic rocks, southwest Sweden: implications for crustal magnetism, J. Geophys. Res., 106(B12), 30523-30546.

McEnroe, S. A., B. Carter-Stiglitz, R. J. Harrison, P. Robinson, K. Fabian, and C. McCammon (2008), Magnetic exchange bias of more than 1 Tesla in a natural mineral intergrowth (vol 2, pg 631, 2007), Nature Nanotechnology, 3(1), 58-58.

Moloni, K., B. M. Moskowitz, and E. D. Dahlberg (1996), Domain structures in single-crystal magnetite below the Verwey transition as observed with a low-temperature magnetic force microscope, Geophys. Res. Lett., 23, 2851-2854

Moskowitz, B., Magnetic Force Microscopy: Techniques and Applications, Workshop presented at 2008 International Conference on Rock Magnetism and its Earth Science Applications, Institut d'Études Scientifiques de Cargèse, France, June 2-7 2008.

Muxworthy, A. R., and W. Williams (2006), Observations of viscous magnetization in multidomain magnetite, J. Geophys. Res., B, 111(B01103), doi:10.1029/2005JB003902.

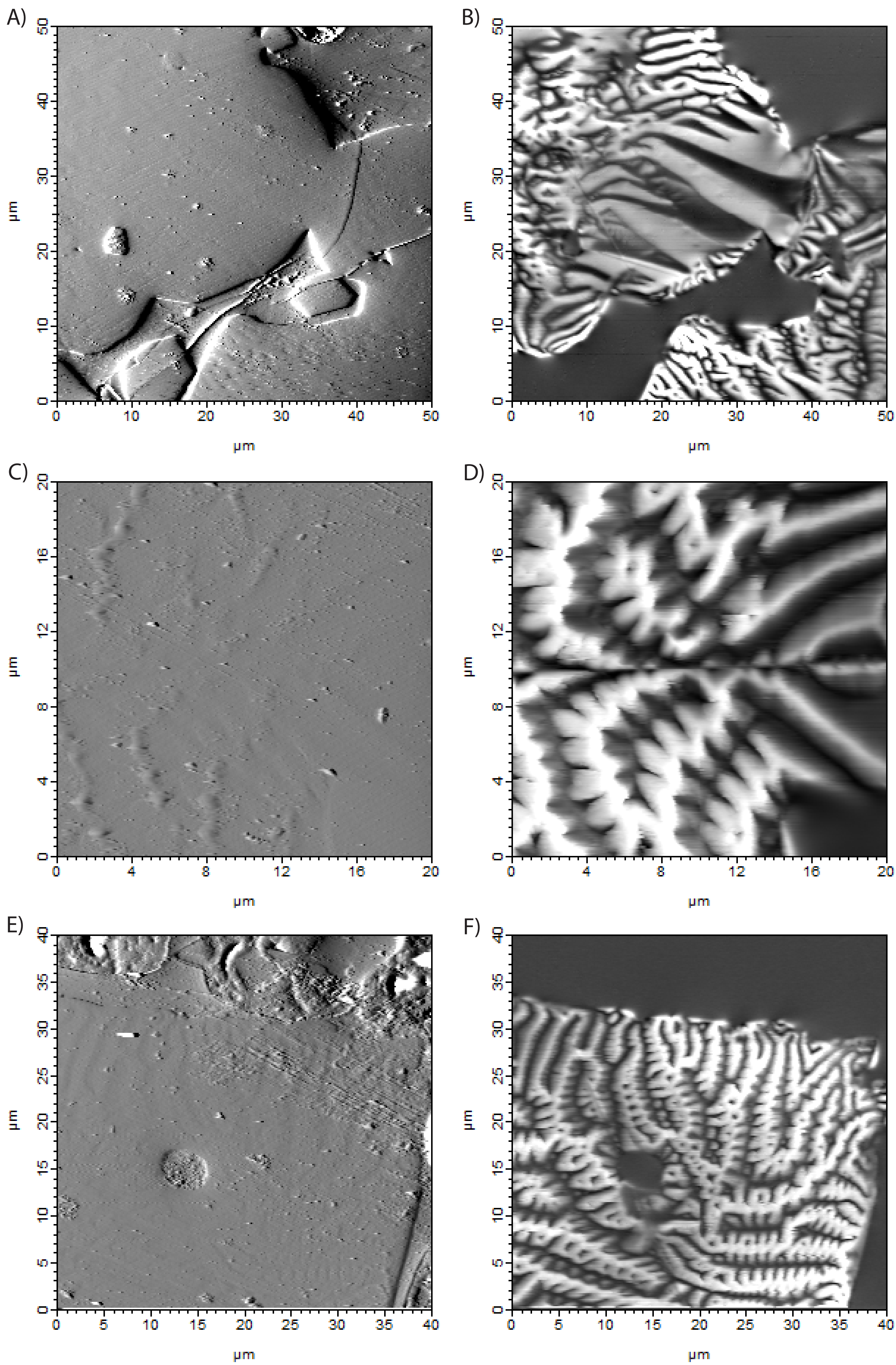

Fig 8. MFM topographic (tap and lift mode) and magnetic images of Mount St. Helens Ti-magnetite crystals.

University of Minnesota
291 Shepherd Laboratories
100 Union Street S. E.
Minneapolis, MN 55455-0128
phone: (612) 624-5274
fax: (612) 625-7502
e-mail: irm@umn.edu
www.irm.umn.edu

The IRM Quarterly

The *Institute for Rock Magnetism* is dedicated to providing state-of-the-art facilities and technical expertise free of charge to any interested researcher who applies and is accepted as a Visiting Fellow. Short proposals are accepted semi-annually in spring and fall for work to be done in a 10-day period during the following half year. Shorter, less formal visits are arranged on an individual basis through the Facilities Manager.

The *IRM* staff consists of **Subir Banerjee**, Professor/Founding Director; **Bruce Moskowitz**, Professor/Director; **Joshua Feinberg**, Assistant Professor/Associate Director; **Mike Jackson, Peat Sølheid** and **Dario Bilardello**, Staff Scientists.

Funding for the *IRM* is provided by the **National Science Foundation**, the **W. M. Keck Foundation**, and the **University of Minnesota**.

The *IRM Quarterly* is published four times a year by the staff of the *IRM*. If you or someone you know would like to be on our mailing list, if you have something you would like to contribute (*e.g.*, titles plus abstracts of papers in press), or if you have any suggestions to improve the newsletter, please notify the editor:

Dario Bilardello
Institute for Rock Magnetism
University of Minnesota
291 Shepherd Laboratories
100 Union Street S. E.
Minneapolis, MN 55455-0128
phone: (612) 624-5274
fax: (612) 625-7502
e-mail: dario@umn.edu
www.irm.umn.edu

University of Minnesota